

## 基于柔性 1,4-苯二硫乙酸配体构筑的二维锰配合物的合成、晶体结构及磁性

王晓娟 尹建玲 陈 静 冯云龙\*

(浙江师范大学物理化学研究所, 浙江省固体表面反应化学重点实验室, 金华 321004)

**摘要:** 水热法合成了一个基于 1,4-苯二硫乙酸( $H_2L$ )柔性配体的  $Mn(II)$  配合物  $[Mn_3L_3(phen)_2]_n$ , 并通过元素分析, 红外光谱、热失重和 X-射线单晶衍射实验对其结构进行了表征。结构分析表明, 配合物是一个包含三核锰结构单元的二维层面结构。对配合物的变温磁化率研究表明, 在三核锰离子间存在弱的反铁磁交换作用。

**关键词:**  $Mn(II)$  配合物; 水热合成; 1,4-苯二硫乙酸; 晶体结构; 磁性

**中图分类号:** O614.7+11 **文献标识码:** A **文章编号:** 1001-4861(2011)02-0367-05

## A New 2D Layer Manganese(II) Complex Assembled by Flexible 1,4-Benzenebis(thioacetic acid) Ligand: Synthesis, Crystal Structure and Magnetic Property

WANG Xiao-Juan YIN Jian-Ling CHEN Jing FENG Yun-Long\*

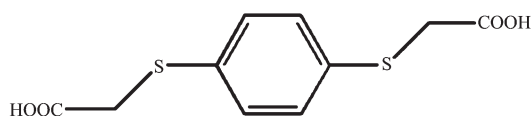
(Zhejiang Key Laboratory for Reactive Chemistry on Solid Surfaces,  
Institute of Physical Chemistry, Zhejiang Normal University, Jinhua, Zhejiang 321004, China)

**Abstract:** A new  $Mn(II)$  complex based on 1,4-benzenebis(thioacetic acid) ( $H_2L$ ),  $[Mn_3L_3(phen)_2]_n$  (**1**, phen=1,10-phenanthroline), has been hydrothermally synthesized and characterized by single crystal X-ray diffraction, elemental analysis, IR spectrum, and TG analysis. The structure can be considered as a two-dimensional (2D) layered architecture which consists of linear trinuclear  $Mn(II)$  units. The magnetic susceptibility data are interpreted with the linear trinuclear law, yielding  $J$  and  $g$  values of  $-1.95(5) \text{ cm}^{-1}$  and 1.98(1). The exchange integral ( $J$ ) indicates a weak antiferromagnetic interactions in the linear trinuclear  $Mn(II)$  unit. CCDC: 734943.

**Key words:**  $Mn(II)$  complex; hydrothermal synthesis; 1,4-benzenebis(thioacetic acid); crystal structure; magnetic property

The design and synthesis of novel polymeric complexes has developed rapidly in recent years due to their potential applications in some fields, such as gas storage, size- and shape-selective catalysis, material science, medicine and magnetochemistry, as well as their intriguing variety of architectures and topologies<sup>[1-9]</sup>. In contrast to the great deal of work on hydrothermal synthesis with phenylene diacetate ligands<sup>[10-14]</sup>, there have been few reports of studies on phenylene

dithioacetate ligands<sup>[15-17]</sup>. Hence, we designed a multi-carboxylate ligand, 1,4-benzenebis (thioacetic acid) ( $H_2L$ , Scheme 1), on the basis of the 1,4-benzenebisoxoacetate<sup>[14,18]</sup> and phenylthioacetate<sup>[19]</sup>. The  $-S-CH_2-$  groups make  $H_2L$  ligand more flexible in comparison with the corresponding benzene-dicarboxylate, while the existence of the benzene ring also provides a rigid element. Recently, we have synthesized some complexes that contain first row transition metal cations

Scheme 1 Molecular structure of  $H_2L$  ligand

bridged by  $H_2L$  and bipyridine analogues ligands<sup>[20-21]</sup>. Moreover, manganese ions not only have versatile coordination behavior but also with well magnetism. Herein, we report the synthesis, structural characterizations and magnetic property of a new Mn(II) complex,  $[Mn_3L_3(phen)_2]_n$  (**1**).

## 1 Experimental

### 1.1 Materials and general methods

All solvents and starting materials for the synthesis were purchased commercially without further purification.  $H_2L$  was obtained according to a rational procedure by 1,4-benzenedithiol<sup>[17]</sup>. The complex was obtained under hydrothermal reaction in a 25 mL Teflon-lined stainless steel Parr bomb. Data collection was performed on a Bruker SMART APEX II CCD diffractometer with Mo  $K\alpha$  radiation ( $\lambda=0.071\ 073\ \text{nm}$ ). Elementary analysis was performed on a EuroEA3000 element analyzer. IR spectrum was measured in KBr pellets on a Nicolet 5DX FTIR spectrometer. Thermogravimetric analysis (TGA) was performed at a rate of  $10\ ^\circ\text{C}\cdot\text{min}^{-1}$  under oxygen stream using a Netzsch STA449C apparatus. The magnetic measurement was carried out with a MPMS SQUID magnetometer Quantum Design SQUID MPMS XL-7 instruments working in the temperature range of 2~300 K at an

applied field of 0.1 T.

### 1.2 Synthesis of $[Mn_3L_3(phen)_2]_n$

A mixture of  $H_2L$  (0.103 g, 0.4 mmol),  $MnCl_2\cdot 4H_2O$  (0.079 g, 0.4 mmol), 1,10-phen (0.040 g, 0.2 mmol), and NaOH (0.032 g, 0.8 mmol) in  $H_2O$  (18 mL) was placed in a Teflon-lined stainless steel vessel and heated at  $160\ ^\circ\text{C}$  for 72 h, then cooled to room temperature over 3 d. Block pink crystals of **1** were obtained and washed with water, dried in air (yield 48%). Anal. Calcd. for  $C_{54}H_{40}Mn_3N_4O_{12}S_6$ (%): C, 50.12; H, 3.12; N, 4.33; S, 14.86. Found(%): C, 50.08; H, 3.08; N, 4.45; S, 14.69. IR (KBr,  $\text{cm}^{-1}$ ): 3 445, 2 930, 1 601, 1 385, 1 209, 1 113, 847, 736, 680, 599, 488.

### 1.3 X-ray crystallography

The diffraction data were collected on a Bruker SMART APEX II CCD diffractometer equipped with a graphite-monochromatized Mo  $K\alpha$  radiation ( $\lambda=0.071\ 073\ \text{nm}$ ) at 296 (2) K. Intensity data were corrected by Lorentz-polarization factors and empirical absorption. The structure was solved with direct methods and expanded with difference Fourier techniques. Except the hydrogen atoms on oxygen atoms were located from the difference Fourier maps, the other hydrogen atoms were generated geometrically. All calculations were performed using SHELXS-97<sup>[22]</sup> and SHELXL-97<sup>[23]</sup> program package. In the title complex, part of  $L^{2-}$  ligands are disordered over two positions in 0.60:0.40 ratio. Further details for structural analyses are summarized in Table 1, selected bond lengths and angles are listed in Table 2.

CCDC: 734943.

Table 1 Crystal data and structure refinement for the complex

Empirical formula	$C_{54}H_{40}Mn_3N_4O_{12}S_6$	$D_c / (\text{g}\cdot\text{cm}^{-3})$	1.632
Formula weight	1 294.08	$\mu / \text{mm}^{-1}$	1.015
Color	Pink	$F(000)$	2 636
Crystal system	Monoclinic	$\theta_{\min} \theta_{\max} / (^\circ)$	1.80, 27.46
Space group	$C2/c$	Reflections collected / uniques / $R_{\text{int}}$	23 347 / 5 996 / 0.043 8
$a / \text{nm}$	1.651 2(7)	Observed reflections ( $I>2\sigma(I)$ )	4 217
$b / \text{nm}$	1.702 3(8)	Parameters refined	421
$c / \text{nm}$	2.040 5(9)	GOF on $F^2$	1.056
$\beta / (^\circ)$	113.28	$R, wR$ ( $I>2\sigma(I)$ )	0.041 2, 0.097 5
$V / \text{nm}^3$	5.268(4)	$R, wR$ (all data)	0.066 1, 0.107 8
$Z$	4	$\Delta\rho_{\max}, \Delta\rho_{\min} / (\text{e}\cdot\text{nm}^{-3})$	580, -512

Table 2 Selected bond lengths (nm) and angles ( $^{\circ}$ ) for the complex

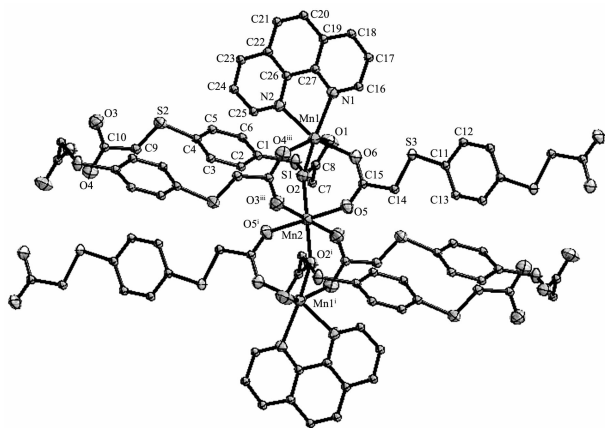
Mn(1)-O(6)	0.209 6(2)	Mn(1)-N(1)	0.222 7(2)	Mn(2)-O(3) <sup>i</sup>	0.216 2(2)
Mn(1)-O(4) <sup>i</sup>	0.211 5(2)	Mn(1)-N(2)	0.225 8(2)	Mn(2)-O(5)	0.216 9(2)
Mn(1)-O(2)	0.219 0(2)	Mn(1)-O(1)	0.248 0(2)	Mn(2)-O(2)	0.217 5(2)
O(6)-Mn(1)-O(4) <sup>i</sup>	103.49(8)	O(4) <sup>i</sup> -Mn(1)-N(2)	88.74(9)	N(2)-Mn(1)-O(1)	84.47(8)
O(6)-Mn(1)-O(2)	95.20(8)	O(2)-Mn(1)-N(2)	97.77(8)	O(3) <sup>i</sup> -Mn(2)-O(3) <sup>ii</sup>	180.0(1)
O(4) <sup>i</sup> -Mn(1)-O(2)	91.81(7)	N(1)-Mn(1)-N(2)	73.74(8)	O(3) <sup>i</sup> -Mn(2)-O(5)	92.66(8)
O(6)-Mn(1)-N(1)	89.06(8)	O(6)-Mn(1)-O(1)	92.64(8)	O(5)-Mn(2)-O(5) <sup>iii</sup>	180.0
O(4) <sup>i</sup> -Mn(1)-N(1)	112.79(8)	O(4) <sup>i</sup> -Mn(1)-O(1)	144.80(8)	O(3) <sup>i</sup> -Mn(2)-O(2)	88.73(8)
O(2)-Mn(1)-N(1)	153.35(7)	O(2)-Mn(1)-O(1)	55.25(7)	O(5)-Mn(2)-O(2)	92.96(6)
O(6)-Mn(1)-N(2)	161.88(8)	N(1)-Mn(1)-O(1)	98.34(8)	O(2)-Mn(2)-O(2) <sup>iii</sup>	180.00(9)

Symmetry transformations used to generate equivalent atoms: <sup>i</sup>  $-x, -y+1, -z$ ; <sup>ii</sup>  $x+1/2, y-1/2, z$ ; <sup>iii</sup>  $-x+1/2, -y+1/2, -z$ .

## 2 Results and discussion

### 2.1 Crystal structure

Single-crystal X-ray diffraction analysis revealed that the title complex is a 2D layer structure containing linear trinuclear Mn(II) units. As shown in Fig.1, it consists of the trinuclear  $[\text{Mn}_3(\mu_2\text{-COO})_6]$  unit, in which Mn(2) atom lies a crystallographic center at (0.25, 0.25, 0), and is six-coordinated by carboxylic O atoms from six different  $\text{L}^{2-}$  ligands (Mn(2)-O 0.217 5(2), 0.216 2(2), 0.216 9(2) nm) to form an octahedral geometry. The Mn(1) is six-coordinated by four O atoms from three  $\text{L}^{2-}$  ligands (Mn(1)-O 0.248 0(2), 0.219 0(2), 0.211 5(2), 0.209 6(2) nm), and two N atoms from one phen molecule (Mn(1)-N 0.222 7(2) and 0.225 8(2) nm) to form a distorted octahedral geometry. Each pair of



Symmetry transformations used to generate equivalent atoms: <sup>i</sup>  $-x, -y+1, -z$ ; <sup>ii</sup>  $x+1/2, y-1/2, z$ ; <sup>iii</sup>  $-x+1/2, -y+1/2, -z$ ; H atoms are omitted for clarity

Fig.1 Coordination environment of trinuclear Mn(II) unit

Mn(II) atoms is  $\mu$ -linked by three carboxylic groups of the individual  $\text{L}^{2-}$  ligands with Mn(1)···Mn(2) distances of 0.362 6(1) nm. The structure is similar to those found in  $[\text{Mn}_3(\text{ppe})_2(\text{OAc})_6]^{[24]}$ ,  $[\text{Zn}_3\text{L}_3(2,2'\text{-bipy})_2]^{[20]}$ , and  $[\text{Co}_3(\text{OAc})_8]^{[25]}$ .

As illustrated in Fig.2, the trinuclear  $[\text{Mn}_3(\mu_2\text{-COO})_6]$  units are joined by flexible carboxyl O atoms to generate 2D networks. Notably, in this 2D layer, it consists of two kinds of link modes: single-stranded along  $b$  axis and double-stranded mode along  $c$  axis. To better understand this structure, the linear trinuclear Mn(II) units serve as nodes, and the nodes are linked by carboxylic O atoms of  $\text{L}^{2-}$  ligands, resulting in a 2D (4, 4) net in the  $ab$  plane.

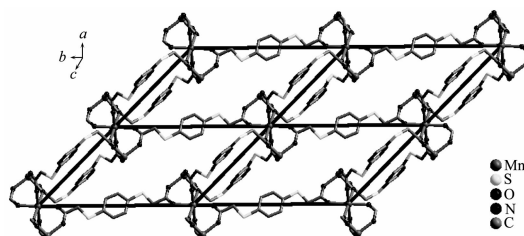


Fig.2 2D (4, 4) net in  $ab$  plane

### 2.2 Magnetic property

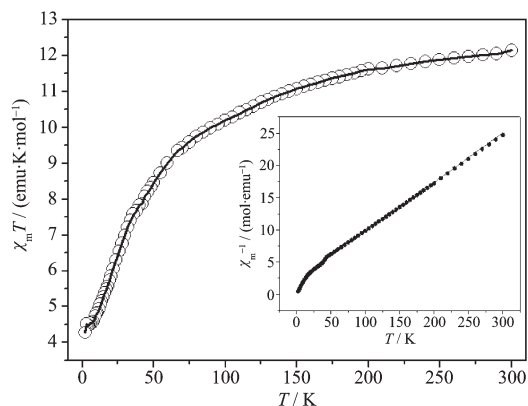
From the magnetic point of view, the title complex can be considered as a linear trinuclear Mn(II) system. The magnetic behaviour of the title complex is illustrated in Fig.3 by means of the magnetic susceptibility ( $\chi_m T$ ) vs the temperature ( $T$ ). The  $\chi_m T$  value per  $\text{Mn}_3$  gradually decreases from  $12.18 \text{ cm}^3 \cdot \text{mol}^{-1} \cdot \text{K}$  at 300 K to  $4.25 \text{ cm}^3 \cdot \text{mol}^{-1} \cdot \text{K}$  at 0.85 K. The  $\mu_{\text{eff}}$  value ( $9.87 \mu_B$ ) at room temperature is smaller than

that of  $10.25\mu_B$  expected for three independent Mn(II) ions with  $S=5/2$ . This result reveals the overall antiferromagnetic character of the system. The Heisenberg spin Hamiltonian model for the isotropic magnetic exchange interaction in the linear trinuclear Mn(II) unit is given in  $H=-2J(S_2S_1+S_2S_3)-2JS_{11}S_1S_3$ , where  $S_1=S_2=S_3=5/2$ ,  $J_{11}=0$  and the numbering has been employed in Fig.1. Take into account the fact that the magnetic coupling except  $Mn_3$  unit is weak, using the contributions of intermolecular force in the fit. Then the temperature dependence of the magnetic susceptibility is given by the equation:

$$\chi_m = \frac{\chi_i}{1 - \chi_i \frac{2zJ'}{Ng^2\beta^2}}$$

$$\chi_i = \frac{Ng^2\beta^2}{2kT} \cdot \frac{A}{B}$$

$A=35+84e^{5x}+35e^{-2x}+10e^{-7x}+165e^{10x}+84e^x+35e^{-6x}+10e^{-11x}+e^{-14x}+286e^{15x}+165e^{4x}+84e^{-5x}+35e^{-12x}+10e^{-17x}+e^{-20x}+455e^{20x}+286e^{7x}+165e^{-4x}+84e^{-13x}+35e^{-20x}+10e^{-25x}+680e^{25x}+455e^{10x}+286e^{-3x}+165e^{-14x}+84e^{-23x}+35e^{-30x}$ ,  $B=6+8e^{5x}+6e^{-2x}+4e^{-7x}+10e^{10x}+8e^x+6e^{-6x}+4e^{-11x}+2e^{-14x}+12e^{15x}+10e^{4x}+8e^{-5x}+6e^{-12x}+4e^{-17x}+2e^{-20x}+14e^{20x}+12e^{7x}+10e^{-4x}+8e^{-13x}+6e^{-20x}+4e^{-25x}+16e^{25x}+14e^{10x}+12e^{-3x}+10e^{-14x}+8e^{-23x}+6e^{-30x}$ .  $x=J/(kT)$ . The best-fit parameters obtained:  $J=-1.95(5) \text{ cm}^{-1}$ ,  $g=1.98(1)$ ,  $zJ'=-0.41(1) \text{ cm}^{-1}$ , and  $R=9.8 \times 10^{-6}$ . The variation of  $\chi_m^{-1}$  also is well described by the Curie-Weiss law in the experimental temperature range 2~300 K with  $C=12.97 \text{ cm}^3 \cdot \text{mol}^{-1} \cdot \text{K}$  and  $\theta=-25.056 \text{ K}$ . The



Solid lines show the best fit under the conditions described in the text

Fig.3 Plots of the  $\chi_m T$  and  $\chi_m^{-1}$  (inset) vs  $T$  for the title complex

negative  $J$  and  $\theta$  values further indicate a weak antiferromagnetic interaction in the linear trinuclear  $Mn_3$  unit. The spin-exchange interaction is comparable to that of the other with the similar structure<sup>[26-28]</sup>.

### 2.3 Thermogravimetric analysis

To study the stability of the title complex, thermogravimetric analytical (TGA) was performed. The TGA curve exhibits two steps of weight losses (Fig. 4). It displays a high thermal stability, as there is no significant weight loss up to 315 °C. An initial weight loss of 30.41% occurred between the temperature range of 315~420 °C corresponds to the removal of two phen molecules (calcd 30.63%). The second weight loss of 58.95% (calcd. 59.81%) in the range of 480~575 °C is consistent with the removal of three  $L^{2-}$  ligands. The remaining products may be  $MnO$ .

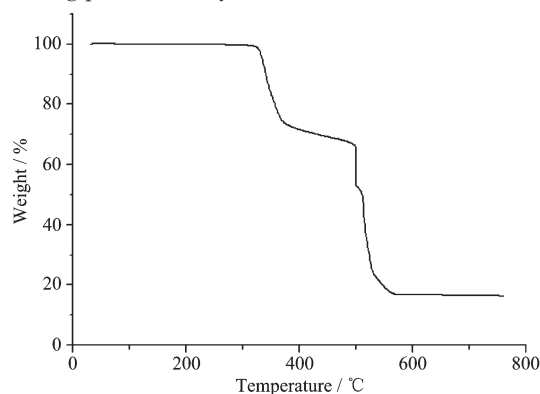


Fig.4 TGA curve of the title complex

In summary, we have successfully synthesized a new Mn(II) complex based on 1,4-benzenebis(thioacetic acid) ligand under hydrothermal conditions. It is a 2D layered architecture which consists of linear trinuclear  $[Mn_3(\mu_2-COO)_6]$  units. Variable temperature magnetic susceptibility indicates the existence of a weak antiferromagnetic interactions in the linear trinuclear unit.

### References:

- [1] Phan A, Doonan C, Uribe-Romo F J, et al. *Acc. Chem. Res.*, **2009**, *43*:58-67
- [2] Lee J Y, Farha O K, Roberts J, et al. *Chem. Soc. Rev.*, **2009**, *38*:1450-1459
- [3] Chen M S, Bai Z S, Okamura T, et al. *CrystEngComm*, **2010**, *12*:1935-1944
- [4] Eddaoudi M, Kim J, Rosi N, et al. *Science*, **2002**, *295*:469-472

- [5] Huh J O, Lee M H, Jang H, et al. *Inorg. Chem.*, **2008**,**47**:6566-6568
- [6] García-Giménez J L, Alzuet G, González-álvarez M, et al. *J. Inorg. Biochem.*, **2009**,**103**:243-245
- [7] Zhao X J, Zhu G S, Fang Q R, et al. *Cryst. Growth Des.*, **2009**, **9**:737-742
- [8] Zhang Z J, Xiang S C, Zheng Q, et al. *Cryst. Growth Des.*, **2010**,**10**:2372-2375
- [9] Moulton B, Lu J J, Zaworotko M J. *J. Am. Chem. Soc.*, **2001**, **123**:9224-9225
- [10] Pan L, Adams K M, Hernandez H E, et al. *J. Am. Chem. Soc.*, **2003**,**125**:3062-3063
- [11] Cotton F A, Lin C, Murillo C A. *Inorg. Chem.*, **2001**,**40**:472-477
- [12] Ren P, Xu N, Chen C, et al. *Inorg. Chem. Commun.*, **2008**,**11**: 730-732
- [13] Zhou J, Sun C Y, Jin L P. *J. Mol. Struct.*, **2007**,**832**:55-62
- [14] Li X F, Han Z B, Cheng X N, et al. *Inorg. Chem. Commun.*, **2006**,**9**:1091-1095
- [15] Gorrane A, Pastor A, Galindo A, et al. *Angew. Chem. Int. Ed.*, **2005**,**44**:3429-3432
- [16] Deivaraj T C, Lai G X, Vittal J J. *Inorg. Chem.*, **2000**,**39**:1028-1034
- [17] Su H, Feng Y L, Wen Y H. *Acta Cryst.*, **2006**,**C62**:m208-m210
- [18] Hong X L, Li Y Z, Hu H M, et al. *Cryst. Growth Des.*, **2006**, **6**:1221-1226
- [19] Sandhu G K, Sharma N, Tiekink E R T. *J. Organomet. Chem.*, **1991**,**403**:119-131
- [20] Yin J L, Feng Y L, Lan Y Z. *Inorg. Chim. Acta*, **2009**,**362**: 3769-3776
- [21] CHEN Jing(陈静), YIN Jing-Ling(尹建玲), WANG Xiao-Juan (王晓娟), et al. *Chinese J. Inorg. Chem. (Wuji Huaxue Xuebao)*, **2010**,**26**:1311-1314
- [22] Sheldrick G M. *SHELXS-97, Program for X-ray Crystal Structure Solution*, Germany, University of Göttingen, **1997**.
- [23] Sheldrick G M. *SHELXL-97, Program for X-ray Crystal Structure Refinement*, Germany, University of Göttingen, **1997**.
- [24] Kang B, Kim M, Lee J, et al. *J. Org. Chem.*, **2006**,**71**:6721-6727
- [25] Reynolds III R A, Dunham W R, Coucouvanis D. *Inorg. Chem.*, **1998**,**37**:1232-1241
- [26] Hsu K F, Wang S L. *Inorg. Chem.*, **2000**,**39**:1773-1778
- [27] Lu X M, Li P Z, Wang X T, et al. *Polyhedron*, **2008**,**27**:3669-2673
- [28] Wang M, Ma C B, Wang H S, et al. *J. Mol. Struct.*, **2008**,**873**: 94-100